Published online 10 April 2007

Nucleic Acids Research, 2007, Vol. 35, No. 8 ***2695–2704***
doi:10.1093/nar/gkm153

HIV controls the selective packaging of genomic, spliced viral and cellular RNAs into virions through different mechanisms

Laurent Houzet[1], Jean Christophe Paillart[2,†], Fatima Smagulova[1,†], Stephan Maurel[1], Zakia Morichaud[1], Roland Marquet[2] and Marylène Mougel[1,*]

[1]CPBS, UMI, CNRS, 4 bd Henri IV, CS 69033, 34965 Montpellier, France and
[2]Architecture et Réactivité de l'ARN, Université Louis Pasteur, CNRS, IBMC, 15 rue R. Descartes, 67084 Strabourg, France

Received January 18, 2007; Revised February 27, 2007; Accepted February 28, 2007

ABSTRACT

In addition to genomic RNA, HIV-1 particles package cellular and spliced viral RNAs. In order to determine the encapsidation mechanisms of these RNAs, we determined the packaging efficiencies and specificities of genomic RNA, singly and fully spliced HIV mRNAs and different host RNAs species: 7SL RNA, U6 snRNA and GAPDH mRNA using RT-QPCR. Except GAPDH mRNA, all RNAs are selectively encapsidated. Singly spliced RNAs, harboring the Rev-responsible element, and fully spliced viral RNAs, which do not contain this motif, are enriched in virions to similar levels, even though they are exported from the nucleus by different routes. Deletions of key motifs (SL1 and/or SL3) of the packaging signal of genomic RNA indicate that HIV and host RNAs are encapsidated through independent mechanisms, while genomic and spliced viral RNA compete for the same *trans*-acting factor due to the presence of the 5′ common exon containing the TAR, poly(A) and U5-PBS hairpins. Surprisingly, the RNA dimerization initiation site (DIS/SL1) appears to be the main packaging determinant of genomic RNA, but is not involved in packaging of spliced viral RNAs, suggesting a functional interaction with intronic sequences. Active and selective packaging of host and spliced viral RNAs provide new potential functions to these RNAs in the early stages of the virus life cycle.

INTRODUCTION

The full-length HIV-1 genomic RNA (FL RNA) is a capped and polyadenylated Pol II transcript that is selectively incorporated into the viral particles as a non-covalent dimer. RNA packaging into virus particles is dependent upon specific interaction between FL RNA and the nucleocapsid protein (NC) domain of the Gag precursor. A recent study suggests that capture of FL RNA occurs at a perinuclear/centrosomal site (1). Selection of the HIV-1 genomic RNA involves the so-called Psi region located immediately upstream of the *gag* start codon (Figure 1) and folded into four stem-loops important for genome packaging (SL1 to SL4) [for review see (2)] (Supplementary Figure 1). In particular, SL1 contains the dimerization initiation site (DIS), a GC-rich loop that mediates *in vitro* RNA dimerization through kissing-complex formation, presumably a prerequisite for virion packaging of FL RNA [for review see (3)]. While both SL2 and SL3 bind HIV-1 NC with high affinity (4), only SL3 seems capable of independently directing the packaging of heterologous RNAs (5), pointing at a particular contribution of SL3 in packaging.

Additional *cis*-acting sequences have also been shown to contribute to FL RNA packaging. Some of these elements are located in the first 50 nt of the *gag* gene, including SL4 (Supplementary Figure 1) and are present only in the FL RNA molecule (6,7), whereas others are located upstream of the splice-donor site (SD1), and are consequently present in all HIV-1 RNAs. These upstream sequences include TAR (*trans*-acting responsive element), poly(A) and U5-PBS hairpins (Supplementary Figure 1) that are involved in FL RNA packaging (8–10).

Although selective encapsidation of FL RNA is largely attributed to Psi, presence of spliced viral RNAs has been found in infectious wild-type (wt) HIV particles (11) and

*To whom correspondence should be addressed. Tel: +33 4 67 60 02 32; Fax: +33 4 67 60 44 20; Email: mmougel@univ-montp1.fr
†The authors wish it to be known that, in their opinion, the second and third authors should be regarded as joint second Authors.

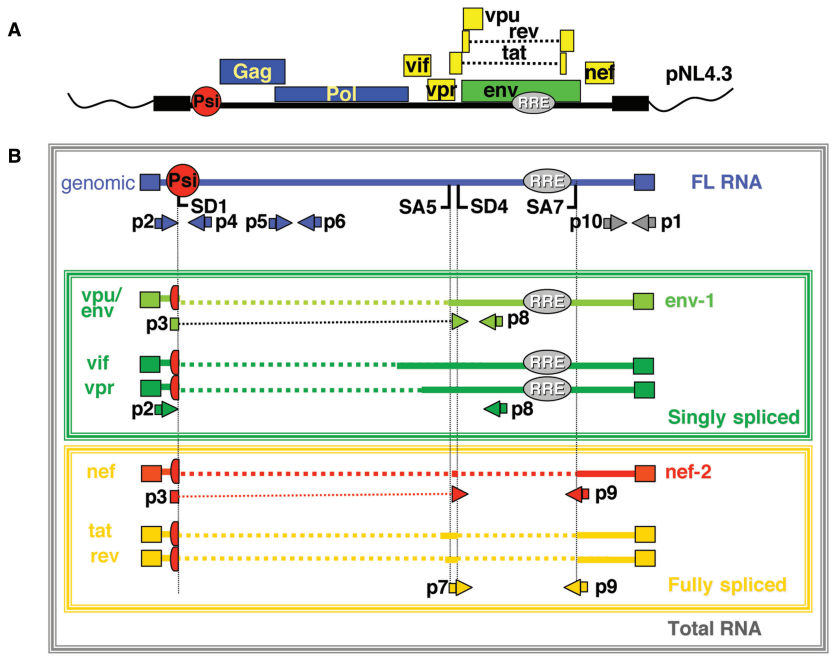

Figure 1. HIV-1 genome expression. (**A**) HIV-1 proviral DNA (pNL4.3). Black boxes correspond to 5′ and 3′ LTR and color boxes to open reading frames. The packaging signal (Psi) in red and the rev-responsive element (RRE) in gray, are also depicted. (**B**) Representation of the major HIV-1 mRNAs species. Spliced RNAs are classified into two groups: the singly and fully spliced mRNAs. Thick lines correspond to exons and dotted lines to introns. Only the two splice donor sites (SD1 and SD4) and the two splice acceptor sites (SA5 and SA7) important for this study are indicated. While p10 + p1, p7 + p9 and p2 + p8 PCR-primer pairs are used to quantify total viral RNAs (gray rectangle), FSpl RNAs (orange rectangle) and singly spliced RNAs (dark green rectangle), respectively, individual RNA species were detected with p2 + p4 or p5 + p6 (FL RNA, blue), p3 + p8 (env-1, light green), and p3 + p9 (nef-2, red).

in mutant particles with altered levels of FL RNA due to Gag or Psi mutations (12–16), but the determinants and mechanism involved in spliced-RNA encapsidation remain undefined.

The FL-HIV-1 transcript undergoes complex alternative splicing that produces >46 spliced RNAs (17), divided in to two classes: fully spliced mRNAs (2.4 kb) encoding Tat, Rev and Nef, and singly spliced mRNAs (4 kb) encoding Vpu, Vpr, Vif and Env (Figure 1). The fully spliced RNAs, also called the early transcripts, follow the classical route of host mRNAs nuclear export. In contrast, singly spliced HIV-1 mRNA and FL RNA are intron-containing transcripts that would normally be restricted from leaving the nucleus, but are exported via the CRM1-dependent protein export pathway due to the HIV-1 Rev protein, which serves as an adaptor between the Rev-responsive element (RRE) present in the *env* gene (Figure 1) and CRM1 (18). Thus, the export pathway might also contribute to the selective packaging of FL RNA. Currently, the packaging efficiency and selectivity of the two groups of spliced RNAs is not well characterized, and one cannot discard the possibility that these spliced viral mRNAs are randomly packaged, together with cellular RNAs.

Indeed, retroviruses package significant amounts of cellular RNA (~50% of the RNA mass in virions) (19). Recently, Telesnitsky and coworkers showed that host 7SL RNA, a component of signal recognition particles (SRPs) essential for protein translocation across the endoplasmic reticulum, is selectively enriched in HIV-1 particles (20). Ribosomal RNA, tRNA or U6 spliceosomal RNA have also been detected in other retroviral particles (21,22), raising the issue of specific packaging determinants.

In order to unravel the mechanisms conferring RNA packaging specificity, we undertook a detailed quantitative analysis of the RNA content of HIV-1 particles by RT-QPCR. Our study not only quantified the relative packaging efficiency of all singly and fully spliced viral mRNAs and of few distinct host RNA species (7SL, U6 and GAPDH RNAs) relative to that of FL RNA, but also allowed to evaluate the importance of the different regions of HIV-1 RNA and of the RNA export pathway on the packaging efficiency. We also studied the effects of SL1 and/or SL3 deletion on the packaging efficiency of these RNAs. By measuring the effects of these deletions on the packaging efficiency of each RNA species, we could not only evaluate the relative importance of SL1 and SL3 in the packaging of FL RNA, but also deduce whether the same mechanism underlies encapsidation of the different RNAs. Altogether, our results allowed us to propose a model for selective RNA encapsidation, revealing a new potential of the RNA structural domains located upstream of Psi and shared by spliced and unspliced RNAs.

MATERIALS AND METHODS

The HIV-1 pNL4.3 molecular clone was used to generate constructs with deletion of SL1 (pNL4.3 ΔSL1), SL3

(pNL4.3 ΔSL3) or both SL1 and SL3 (pNL4.3 ΔSL1SL3). To obtain these constructs, the QuickChange site-directed mutagenesis kit was used according to the manufacturer (Stratagene), using plasmid DNA pLTR5′-NL4.3 containing the AatII-SphI fragment of pNL4.3 molecular clone (23). The mutated oligonucleotides were pS681-746 (5′-TCTCTCGACGCAGGAGGGCGGCGA CTGGTG-3) and pAS681-746 (5′-CACCAGTCGCCGC CCTCCTGCGTCGAGAGA-3′) for mutant pLTR5′-ΔSL1 and pS751-794 (5′-CGCCAAAAATTTTGAAAG GAGAGAGATGGG-3′) and pAS-751-794 (5′-CCCATC TCTCTCCTTTCAAAATTTTTGGCG-3′) for mutant pLTR5′-ΔSL3. After confirmation of the presence of the deletion by restrictions and DNA sequencing, plasmid DNAs were digested with AatII and SphI and the resulting fragment was substituted for the homologous region of pNL4.3 DNA. Positions of deletions are given in Supplementary Figure 1.

Cell culture, transfections and infections

Human embryonic kidney 293 (HEK 293T) cells were maintained at 37°C in Dulbecco's modified Eagle's medium (DMEM) supplemented with glutamine (2 mM), penicillin, streptomycin and 10% (v/v) heat-inactivated fetal calf serum. The human T lymphoblastoid H9 cell lines were grown in RPMI 1640 medium supplemented the same way. Transfections of 293T cells were performed with 3×10^6 cells splitted the day before in 100-mm dishes in 8 ml medium by calcium phosphate precipitation. For moderate- or high-level expression of HIV, 2 μg along with 6 μg of carrier DNA (plasmid pSP72) or 8 μg of HIV-1 plasmid DNA were transfected and samples collected 20 or 48 h after transfection, respectively. For cotransfections, 2 μg of each plasmid were used along with 4 μg of pSP72 carrier. In all cases, cells were splitted and washed with PBS a few hours after transfection to eliminate plasmid excess. The amount of HIV particles in supernatants was determined using a HIV-1 CA p24 core antigen enzyme-linked immunosorbent assay (ELISA) Kit (Beckman Coulter™). Virus-containing supernatants used for infection of H9 cells were obtained with 8 μg HIV-1 plasmid DNA. To assess the viral titers of wt and mutant viruses, H9 cells were infected with serial dilutions of cell-free medium harvested from transfected 293T culture. Cells were fed every 3–4 days. Viral replication was monitored over 10 days by standard RT enzyme assay (24).

RNA extraction and analysis

RNA extractions from cell and virion were performed as previously described (25). To control virion-RNA extraction from the virus-containing supernatants, 5 μl of supernatant of MuLV-infected NIH3T3 cells, previously calibrated as in (26), were added as a tracer to each HIV supernatant before ultracentrifugation. Usually, a maximal variation of 20% was found which was corrected accordingly. Reverse transcription was performed as described (25) with 1 μg of total cellular RNA or 1/20 aliquots of virion RNA samples. Oligo(dT) was used as RT-primer for all viral and GAPDH mRNAs while reverse transcription of 7SL and U6 RNAs required specific internal primers. Standard PCR was performed with 5% of RT reaction, using Takara Taq (Invitrogen). Quantitative PCR was achieved with 2.5% of the RT-d(T), 0.125% of RT-U6 and 0.05% of RT-7SL reactions with SYBR Green Kit (Roche) with the LightCycler (Roche) and RotorGene (Labgene) systems. A standard curve was generated from 50 to 500 000 copies of pNL4.3 plasmid. Each RT-PCR assay was accompanied by controls without reverse transcriptase that showed DNA contamination levels <0.1% of the HIV genomic RNA, and <0.001% of 7SL and U6 RNAs. Packaging efficiency was determined by calculating the ratio of the total amount of each RNA present in the supernatant (V) and the total amount present in cells (C). All primer sequences and detailed PCR conditions will be provided on request.

RESULTS

Detection of singly spliced viral RNAs in HIV-1 particles

Besides specific packaging of two copies of FL RNA, HIV-1 also incorporates spliced viral RNAs, although at a lesser extent (11,12). First, we looked for virion-associated singly spliced RNAs, including the env mRNA present in all retroviruses. RNA samples were extracted from pNL4.3-transfected cells and from viral pellets obtained from cell culture supernatants, and analyzed by standard RT-PCR as described in the Materials and methods section. The primer combination p2 + p8 enabled simultaneous detection of all singly spliced RNAs (Figure 1). The most abundant singly spliced HIV-1 RNAs in cells were vif-2 (1347 nt), vpr-3 (870 nt) and env-1 (284 nt) (Figure 2A, lane 1). A similar pattern was observed with RNA samples extracted from viral pellet (Figure 2A, lane 4). FL RNA was detected with primers p2 + p4 (Figure 2A, lanes 1 and 4). By comparison with the singly spliced RNAs, FL RNA was enriched in the viral particles, as expected from its preferential packaging. In all cases, no background signal was observed with mock-transfected cells (Figure 2A and B, lanes 3 and 6). A positive control corresponding to direct PCR amplification with pNL4.3 displayed a specific FL signal with p2 + p4 primers (Figure 2B, lane 8), while no signal was observed with the p2 + p8 primers, specific for the spliced RNA species (Figure 2A, lane 8). Thus, our results confirm the presence of at least the most abundant singly spliced RNA species, and probably all, in wt HIV-1 particles, and suggest that all singly spliced viral RNAs are packaged with similar efficiencies.

Quantitative and comparative analysis of viral FL, singly and fully spliced RNA packaging

Up to now, there are no data available on spliced viral RNA packaging efficiency in HIV-1 particles. Indeed, the low abundance and large diversity of the HIV-1-spliced transcripts make difficult their quantification in virions. Here, we used several primer pairs allowing specific analysis of one major representative of each HIV spliced RNA classes: env-1, representing 74% of the singly spliced

RNAs, and nef-2, amounting to 27% of all fully spliced RNAs (17) (Figure 1). In addition, we designed a primer pair specific for the SD4/SA7 exon–exon junction (p7 + p9, Figure 1) that allowed overall quantification of the fully spliced RNA class (FSpl).

Since it was previously reported that levels of spliced HIV RNAs varied between different infected cell types (PBMC, macrophages or T-lymphocytes) and with the kinetics of infection (27), transfection, although less physiological than infection, was used in this study. Nevertheless, moderate-level expression of HIV-1 was chosen to prevent cell lysis, which could disturb the intracellular RNA traffic (28). Quantitative analysis of HIV FL, env-1, nef-2 and FSpl RNAs were performed from the same RT reaction using oligo d(T) as a primer, followed by specific QPCR amplifications. The amplification products were analyzed on agarose gel (Supplementary Figure 2A) and sequenced (not shown) to ensure that the expected products were amplified. The copy numbers of each viral RNA in assays and mock controls were measured in 50 ng of total cell RNA and 1/400 of virion RNA, and a representative experiment is shown in Supplementary Figure 2B. To determine encapsidation efficiencies, copy numbers measured in cells and in virions were reported to the total input of cellular and virion RNA samples, and virus-to-cell RNA ratios $[(V/C) \times 100]$ were calculated and normalized to FL level (Figure 3A). As expected, FL RNA was encapsidated more efficiently than spliced viral RNAs (>59-fold). FSpl RNAs, as well as its major representative nef-2 RNA, were incorporated with an efficiency similar to env-1 RNA and likely to all singly spliced RNAs (Figure 2A). These results showed that singly and fully spliced RNAs displayed similar encapsidation capabilities. Considering that the presence of spliced RNA could result from the moderate-level expression of HIV, we conducted similar analysis in high-level expression conditions (see the Materials and methods section). The data are reminiscent of those observed in moderate-level expression conditions with even higher encapsidation levels of spliced RNA (data not shown). Thus, in both moderate- and high-expression conditions, HIV-1 particles contained low but significant amounts of singly and fully spliced viral RNAs.

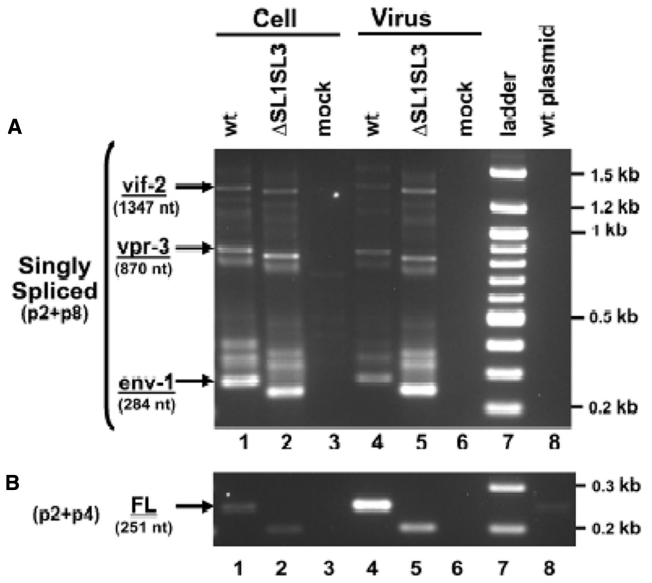

Figure 2. Analysis of unspliced (FL) and singly spliced mRNAs in wt and mutant HIV-1 particles. Singly spliced (**A**) and FL (**B**) RNAs were detected in RNA samples extracted from wt (lanes 1 and 4), ΔSL1SL3 (lanes 2 and 5) and mock (lanes 3 and 6) transfected cells and in corresponding viral particles (lanes 4–6) using standard RT-PCR. As a control, amplification was also performed using pNL4.3 plasmid as a template (lane 8). Bands corresponding to vif-2, vpr-3 and env-1 mRNAs are indicated by arrows. In the mutant virus, all amplicons were shortened by 34 nt, due to the SL1 deletion. This result is representative of at least three independent experiments.

Quantitative analysis of host RNA packaging

Packaging of spliced viral mRNAs may represent fortuitous random packaging. To determine whether packaging of env-1- and nef-2-spliced RNAs is specific, we also evaluated the incorporation levels of several host RNAs. Comparison with 7SL RNA was especially interesting

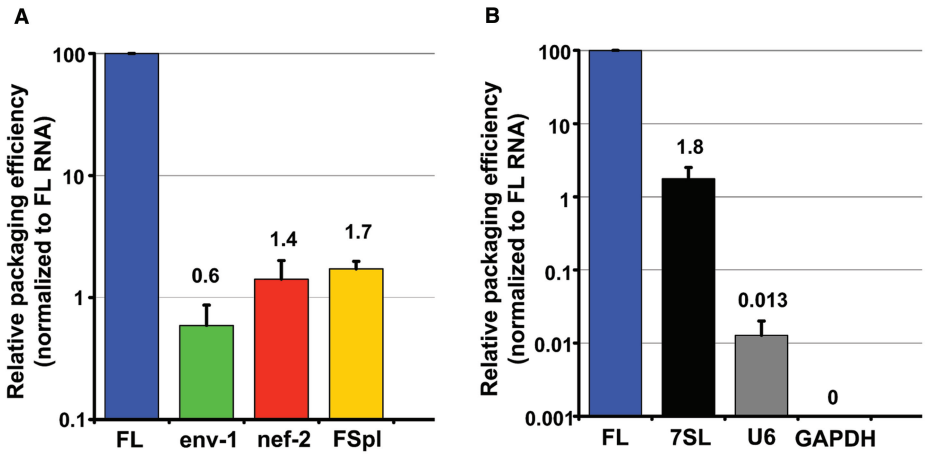

Figure 3. Relative encapsidation efficiencies of HIV-1 (**A**) and total cellular (**B**) RNAs in wt virus. RNAs were quantitated by RT-QPCR in both transfected cell and virus. Relative packaging efficiencies were determined $[(V/C) \times 100]$ and normalized to FL level. Results represent mean ± standard deviations of at least three independent experiments.

because of its preferential packaging into HIV-1 particles (20). Similarly, we monitored nuclear U6 snRNA that was previously described associated to murine leukemia viruses (MLV) (29). As a marker for random packaging, we analyzed incorporation of a housekeeping mRNA abundantly expressed in cells, GAPDH mRNA. These three cellular RNAs were analyzed as the spliced viral RNAs and their copy numbers measured in transfected or mock-transfected cells and in the corresponding supernatants (Supplementary Figure 3). To assess the significance of the presence of these host RNAs in virions, percentages of host RNA leakage were calculated as (total c.p.s. in C/total c.p.s. in V) $\times$ 100 of mock samples. Host RNA leakages were similar for the three host RNAs (0.0037% for U6, 0.0043% for 7SL and 0.0031% for GAPDH). Leakage was subtracted from assays, and encapsidation efficiencies of host RNA were determined as above for spliced RNAs, and normalized to the FL RNA level (Figure 3B). GAPDH mRNA level in the supernatant culture was insensitive to the production of HIV particles, indicating that GAPDH mRNA was not detectably incorporated into HIV virions. The packaging efficiencies of 7SL RNA and U6 snRNA were very different, being 55-fold and >3 orders of magnitude lower than that of viral FL RNA, respectively. These three host RNAs were packaged with even higher efficiencies when HIV-1 was highly expressed (data not shown).

These results show that all cellular RNAs were not encapsidated with the same efficiency, suggesting that they are not randomly packaged. The undetectable GAPDH mRNA level suggests that active mechanisms of packaging and/or exclusion are involved and that the pool of cellular mRNAs is counter-selected.

Effects of Psi mutations on virus release and infectivity

We showed that viral singly and fully spliced RNAs and some host RNAs are natural components of HIV-1 virions. To further understand the mechanisms governing packaging of these RNAs, we altered FL RNA packaging by deleting the two major *cis*-acting Psi elements, SL1 and SL3 (Supplementary Figure 1), either individually or together. A decrease, or a compensatory increase, of the amount of spliced or host RNAs in viral particles in response to diminished FL RNA packaging, would support the existence, or not, of common packaging determinants between these RNAs.

First, we analyzed the impact of these deletions on HIV-1 replication. Mutants HIV-1 molecular clones were transfected into 293T cells to produce virus stocks that were subjected to viral capsid protein analysis by ELISA. As shown in Table 1, deletions did not significantly affect release of capsid proteins, suggesting that similar levels of wt and mutant viral particles were released in the media. Then, same amounts of virus were used to infect H9 cells. H9 progeny viruses were titrated by measuring the RT activity in culture supernatants. Deletion of SL1 resulted in a greater reduction in virus infectivity (200-fold) than deletion of SL3 (4-fold), with a maximal effect for the double deletion mutant, which was essentially non-infectious (Table 1). These alterations would complicate the analysis of the mutation effects in an infection context. These results indicated that both SL1 and SL3 are important for HIV-1 replication but that their deletion did not significantly interfere with virion production.

Table 1. Effect of mutations on virus release, infectivity and splicing

	Wt	ΔSL1	ΔSL3	ΔSL1SL3
p24 in supernatant[a]	100	69 ± 29	70 ± 4	87 ± 37
Infectivity[b]	100	0.5 ± 0.03	24 ± 10	ND
Viral RNA in cells[c]				
Tot/FL	100	93 ± 12	81 ± 14	83 ± 19
env-1/FL	100	97 ± 18	105 ± 17	83 ± 15
nef-2/FL	100	86 ± 14	91 ± 24	72 ± 11
FSpl/FL	100	98 ± 36	81 ± 26	82 ± 17

All results represent mean ± standard deviations of at least three independent experiments. For comparison purposes, averaged values were normalized to wt levels.
[a]Levels of virions released in culture media of 293T cells transfected with wt and mutant constructs were analyzed by quantitation of viral capsid (p24) with p24 ELISA kit.
[b]Virions from (a) were used to infect H9 cells and infectivity was determined by monitoring reverse transcriptase activity in supernatant of infected H9 cells. ND: not detectable.
[c]Total viral RNA (Tot), env-1, nef-2, FSpl and FL RNAs were quantified by specific RT-QPCR in RNA samples extracted from transfected cells and their relative abundance to FL RNA was calculated.

Effects of Psi mutations on viral RNA production

We could not *a priori* exclude an impact of the SL1 and/or SL3 deletions on the very close SD1 site. Because modifications of FL RNA splicing would complicate the analysis of the effects of these deletions on RNA packaging, we first examined the splicing efficiencies of the Psi mutant viruses. RNA samples extracted from transfected 293T cells were analyzed by RT-QPCR to quantify FL, FSpl, nef-2 and env-1 RNA species. Quantification of the total viral RNA pool indicated that wt and mutant RNAs were expressed at similar levels (data not shown) excluding an effect of mutations on viral RNA stability. For comparative purposes, tested RNA-to-FL RNA ratios were determined and normalized to wt levels (Table 1). Our results indicated that neither FSpl, nef-2, nor env-1 RNA levels were modified by the deletions. Thus, deletion of SL1 and/or SL3 preserved FL RNA expression levels without affecting splicing.

Effects of SL1 and/or SL3 deletions on RNA packaging

Genomic RNA levels in virions and virus-producing cells were quantified by RT-QPCR and encapsidation efficiencies were determined for each FL RNA mutant and normalized to that of wt FL RNA (Figure 4A). Deletion of SL3 resulted in a 2-fold reduction of the FL RNA encapsidation efficiency. Deletions of SL1 or SL1 and SL3 had more severe effects, reducing FL RNA packaging 5-fold. Thus, both RNA stem-loops were important for genomic RNA encapsidation, with a major role for SL1.

Next, we examined the consequences of reduced FL RNA incorporation on packaging of the spliced viral RNAs and host RNAs in mutant particles. First, we glanced at the effect of the SL1 + SL3 deletion on the

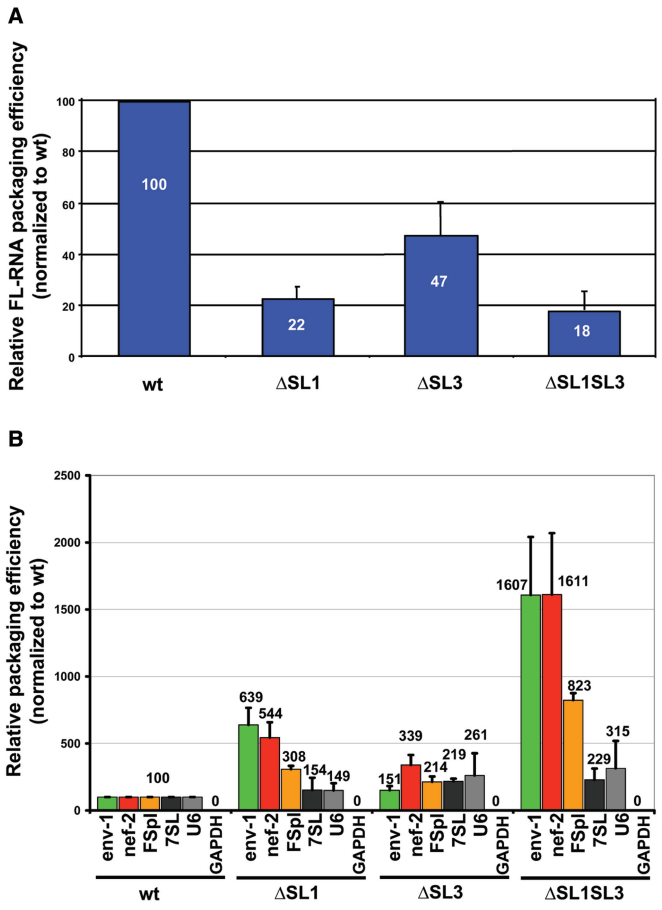

Figure 4. RNA encapsidation efficiencies in mutant viruses. (**A**) Relative encapsidation efficiency of FL RNA. Encapsidation efficiency $[(V/C) \times 100]$ is given as% of the wt level. (**B**) Relative encapsidation efficiency of spliced viral and host RNAs. For each RNA species, packaging efficiencies levels were average (±SD) from at least three independent experiments and normalized to wt level.

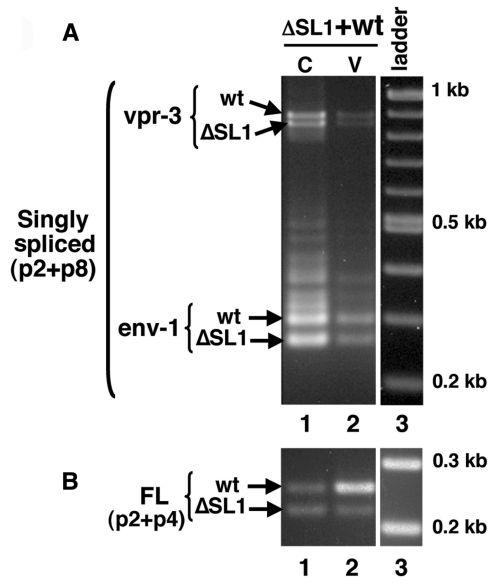

Figure 5. Comparison of viral RNA encapsidation when wt and ΔSL1 viruses are coexpressed. 293T cells were cotransfected with same amount of wt and ΔSL1 constructs. RNA was extracted from cells (C) (lane 1) and viruses (V) (lane 2) and singly spliced (**A**) and FL (**B**) RNAs were detected by RT-PCR. Because ΔSL1 deletion shortened the amplified product by 34 nt, wt and mutant forms of each RNA species were distinct.

FL and the overall profile of singly spliced RNA packaging by standard RT-PCR. While similar levels of wt and mutant RNAs were present in cells, ΔSL1SL3 FL RNA was less efficiently incorporated into virions than wt FL RNA, correlating with quantitative data of Figure 4A, whereas singly spliced RNAs were more abundant in ΔSL1SL3 virions (Figure 2). These results showed that the simultaneous deletion of SL1 and SL3 affects packaging of FL and singly spliced RNAs in opposite ways. Besides, they confirmed that these deletions did not affect splicing, since the relative abundance of singly spliced RNA species was the same in cells expressing wt or ΔSL1SL3 viruses (Figure 2).

Next, detailed quantitative studies of the RNA content of ΔSL1, ΔSL3 and ΔSL1SL3 particles were undertaken by RT-QPCR. Levels of singly and fully spliced viral RNAs, as well as host 7SL, U6 and GAPDH RNAs, were assessed in the same viral pellets as used above for FL RNA analysis. Encapsidation efficiencies of each RNA species were determined for all mutants and normalized to those determined for wt virus (Figure 4B). As observed above with wt virions (Figure 3B), GAPDH mRNA was excluded from all mutant virions. In ΔSL1 virions, a strong increase of all spliced RNA species was observed, with a maximum effect for the env-1 RNA (6-fold). However, deletion of SL1 did not significantly enhance packaging of 7SL and U6 RNAs (Figure 4B). Deletion of SL3 resulted in a slight increase (2-fold) of both spliced viral RNA and host RNA encapsidation levels, revealing similar limited consequences of SL3 deletion on the two RNA species. In contrast, the double mutant (ΔSL1SL3) showed a drastic 16-fold increase of the spliced viral RNAs, accompanied by a modest 2–3-fold increase of 7SL and U6 RNAs in ΔSL1SL3 particles.

In conclusion, no significant difference was observed between the singly and fully spliced RNA encapsidation among the deletion mutants. Interestingly, deletions induced different effects on encapsidation of host and spliced viral RNAs. While 7SL and spliced viral RNAs appeared encapsidated with similar efficiency in wt virions (FSpl = 7SL = 1.8%, Figure 3), they displayed very different packaging efficiencies in ΔSL1 and ΔSL1SL3 particles, strongly suggesting that spliced viral RNAs and 7SL RNA are incorporated through different mechanisms.

Competition between wt and ΔSL1 RNAs for packaging

It is usually thought that the presence of SL1 in HIV-1-spliced RNAs could direct their encapsidation into virions. However, the significant increase of spliced-RNA packaging observed upon SL1 deletion did not favor this hypothesis, and rather suggested an inhibitory effect of SL1 on spliced-RNA packaging. To directly address this issue, we undertook competition experiments. The wt and ΔSL1 pNL4.3 plasmids were cotransfected in 293T cells. RNA was extracted from cells and virions and

analyzed by standard RT-PCR, followed by agarose gel electrophoresis, and visualization of the bands corresponding to vpr-3 and env-1 RNAs. This approach allowed discrimination between wt and mutant RT-PCR products since the latter were shorter, due to SL1 deletion (Figure 5). When wt and ΔSL1 singly spliced RNAs were equally coexpressed in cells, virions exhibited similar levels of the two RNAs (Figure 5A, lanes 1 and 2), indicating that they were incorporated in virions with the same efficiency. Thus, the SL1 motif did not confer any advantage or disadvantage to the singly spliced RNAs for packaging. Of course, SL1 remained a crucial determinant for FL RNA packaging, since wt FL RNA showed preferential incorporation over ΔSL1 FL RNA when wt and ΔSL1 FL RNAs were coexpressed at similar levels in cells (Figure 5B, lanes 1 and 2).

DISCUSSION

The results described in this article indicate that HIV-1 incorporates measurable amounts of nongenomic RNAs such as spliced viral RNAs and cellular 7SL and U6 RNAs in addition to the genomic FL RNA. We examined whether the same mechanism underlies encapsidation of these different RNA species.

Packaging of cellular RNAs greatly varied from one species to another. 7SL RNA was packaged in wt HIV-1 particles as efficiently as singly and fully spliced viral RNAs, whereas packaging of U6 snRNA was less efficient (Figure 3B). At the opposite, GADPH mRNA was not detectably encapsidated into virions, arguing against a background random packaging of cellular RNAs.

When packaging of FL RNA was reduced by deleting SL1 and/or SL3 (Figure 4A), the space normally occupied by genomic RNA was not passively and randomly filled by cellular RNA. Indeed, GAPDH mRNA remained undetectable in the virions containing mutant FL RNA and the relative packaging efficiency of 7SL and U6 RNAs only slightly increased (Figure 4B). In contrast, to compensate the loss of FL RNA, mutant particles specifically favored encapsidation of spliced HIV RNA (see below). These results demonstrate that host and viral RNAs were packaged through independent mechanisms. Consistently, it was recently reported that packaging of 7SL RNA in HIV-1 does require neither the FL RNA nor the Gag protein (20). It is also unclear whether packaging of U6 and 7SL RNAs were governed by the same process. The only common feature between these host RNAs is transcription by RNA polymerase III, which might require common determinants and/or a trafficking pathway contributing to packaging.

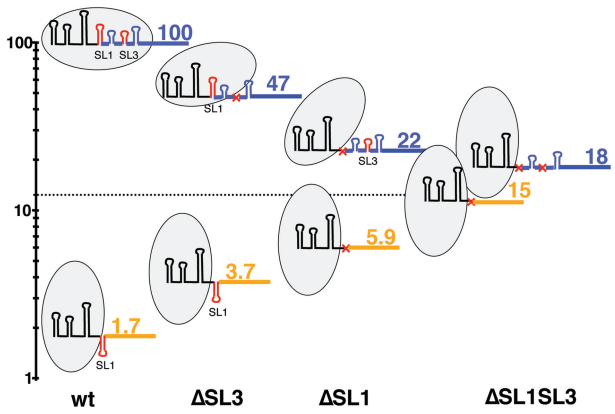

Figure 6. Model for competitive and selective encapsidation of viral unspliced and spliced RNAs. For an overview of RNA packaging variations among mutants, packaging efficiencies of FL (blue) and fully spliced RNA (orange), expressed as% of the wt FL level, were reported in a log-scale graph. The SL1-SL4 hairpins forming the Psi site were schematically drawn, with SL1 and SL3 hairpins in red, along with the three upstream structural motifs: TAR, poly(A) and U5-PBS hairpins in black. The dotted line shows the axial symmetry between FL and spliced RNA variations illustrating a competition between the two RNA species for packaging. Opposite co-variation and convergence are two features suggesting that spliced and FL RNAs compete for a common *trans*-acting factor (oval) that binds the different wt or mutant RNAs with high (horizontal) or medium (vertical) affinity.

Spliced viral RNAs are usually considered to be encapsidated in trace amounts in wt HIV-1 particles. However, our quantitative analysis show that spliced viral RNAs are encapsidated with significant efficiency (Figure 3A). Importantly, we (Houzet *et al*. submitted for publication) and others (11) have shown that spliced mRNAs are reverse transcribed during infection, demonstrating that viral particles containing spliced viral RNAs are infectious. In addition, we did not observe any significant difference in the packaging efficiency of the singly spliced (RRE+) and fully spliced (RRE−) RNAs, indicating that: (i) spliced viral RNAs are equally encapsidated regardless of their nuclear export pathway, (ii) the RRE motif is not involved in spliced-RNA packaging and (iii) there is no packaging determinant in the exonic sequences removed during full splicing but conserved in the singly spliced RNAs.

Whereas deletions of SL1 and/or SL3 had little effect on encapsidation of host RNAs, they favored packaging of both singly and fully spliced viral RNA (Figure 4B). In addition, our quantitative analysis demonstrates a direct correlation between the decrease in packaging efficiency of FL RNA and the increased packaging of FSpl RNAs (Figure 6). This opposite co-variation was observed with all spliced RNA species studied in this work (and not shown in Figure 6) and suggests selective incorporation of spliced viral RNAs via an active mechanism. It also indicates that the FL and spliced viral RNA species are packaged in a competitive manner, thus implying that these RNA species utilize common *cis*-packaging signals and *trans*-protein factor(s).

Remarkably, in mutant ΔSL1SL3 virions, FL and FSpl RNAs were packaged with similar efficiency (Figure 6) suggesting that the 5′ UTR upstream of SL1 contains *cis*-packaging signals, shared by FL and spliced viral RNAs, that are sufficient to confer a packaging efficiency corresponding to 15–18% of the packaging efficiency of wt FL RNA (Figure 6). On the other hand, it suggests that SL2, the putative SL4 and the coding sequences unique to FL RNA marginally contribute to packaging of FL RNA, at least in the context of the ΔSL1SL3 mutant. Interestingly, the region located upstream of SL1 includes three well-characterized structures, TAR, polyA and U5-PBS hairpins, that have been shown to be involved

in FL RNA packaging (8,9,30–33). Since these three structural domains are common to all HIV spliced and unspliced RNAs, they are likely responsible for encapsidation of the viral FL and spliced RNAs in ΔSL1SL3 mutant, which remained selective despite its limited efficiency. Such a contribution of sequences located upstream of Psi is not a general feature of retroviruses, since mutations in MLV Psi virtually abolished encapsidation of FL RNA (34,35) and did not increase spliced RNA levels in MLV particles [(34) and data not shown].

Analysis of the SL1 deletion was of particular interest, since SL1 is present in both FL and spliced wt RNAs. Unexpectedly, this deletion had opposite effects on FL and spliced RNA packaging, with an inhibitory effect on FL RNA and a strong positive effect on spliced RNA packaging (Figures 4 and 6). However, when wt and ΔSL1 viruses were coexpressed, spliced wt and ΔSL1 RNAs were packaged with the same efficiency (Figure 5). Thus, increased packaging of spliced RNA in the ΔSL1 mutant resulted from a competitive compensation of the defect in FL RNA packaging, rather than from a direct *cis*-effect of the deletion on spliced RNA.

Since SL1 has been identified as the DIS of HIV-1 RNA *in vitro* and contribute to dimerization of HIV-1 FL RNA in cell culture [for review see (36)], our results exclude the possibility that spliced viral RNAs are packaged by forming heterodimers via SL1 with the FL genomic RNA. In addition, the absence of stoichiometric co-variation between FL and spliced RNA packaging with the mutants also argues against this possibility. Our results also suggest that spliced viral RNAs do not homodimerize via SL1 in cell culture or that SL1 dimerization of these RNAs does not affect their packaging, in sharp contrast with FL RNA, for which dimerization and packaging are intricately linked processes [for reviews see (2,36)].

In keeping with previous studies performed either with chimeric constructs, or in cotransfection of wt and mutant HIV, or in infection [(37) and references therein], we found that deletion of SL1 and/or SL3 hairpins decreased FL RNA levels in virions, confirming their roles in genomic RNA packaging. Our study indicates that SL1 plays a greater role in RNA packaging and viral infectivity than SL3. Note that the deletions studied in these early studies did not only encompass SL3 or SL1, but larger regions which may indirectly affect packaging by altering folding of the complete Psi region. Interestingly, SL1 appears to favor RNA packaging only in the context of the FL RNA, suggesting that it works together with sequences that are not present in spliced RNA. In particular, sequences in *gag* might directly interact with SL1 since they are known to stabilize the SL1-mediated RNA dimer *in vitro* (38,39). We suggest that these sequences, which remain to be precisely identified, cooperate with SL1 to direct specific packaging of the FL RNA. This would explain why *gag* sequences enhance packaging of wt FL RNA (6,7), but do not seem to contribute to packaging of ΔSL1SL3 FL RNA (Figure 6).

Altogether our observations allow us to propose a working model in which FL and spliced RNAs act as competitors in a common selective but weakly efficient packaging process driven by determinant(s) located upstream of the Psi region. In the wt virus, the presence of Psi insures optimal specificity and efficiency, mainly mediated by SL1, and possibly in cooperation with *gag* sequences, to FL RNA to the detriment of spliced RNAs. This model correlates with previous works showing that the region encompassing SL1 to SL4 is not sufficient to target RNA into HIV-1 virions (40). Instead, the minimal region shown to confer autonomous packaging activity spans the first 350 to 400 bases of the genome, and thus not only includes Psi, but also 242 bases upstream and the 5′ 40 nt of *gag* (6,7,41,42). Our model suggests that the upstream three hairpins also provide low affinity interactions with a *trans*-acting factor, presumably Gag. This hypothesis is supported by a previous study showing that Gag binds the 5′ first 261 nt, precisely corresponding to 5′ leader sequence of spliced RNA, with significant affinity (43). This model does not exclude that other factors might also indirectly affect packaging, such as subcellular localization of the RNA or its ability to bind cellular or viral chaperone proteins (44–46).

A better understanding of the mechanism allowing packaging of HIV-1-spliced RNAs could bring the first elements to explain the alterations of packaging specificity in AIDS patients treated with highly active antiretroviral therapy. Recent plasma analysis of these patients revealed accumulation of defective HIV particles mainly containing spliced viral RNAs (47).

In conclusion, active packaging of nongenomic RNAs likely increases the probability of generating recombinant transforming viruses through a reverse-transcriptase-mediated mechanism (19). Since evidence of reverse transcription of spliced viral mRNAs and host 7SL and U6 RNAs has been reported (11,21,48), their selective encapsidation could have profound effects on the malignant transformation process of infected cells. These considerations should be taken into account in gene therapy strategies that commonly used HIV-based vectors or HIV-producer cells (49). Avoiding possible inadvertent packaging is indeed a major concern in these approaches. Thus, understanding of the packaging specificity should help in designing optimal vectors and packaging cell lines.

SUPPLEMENTARY DATA

Supplementary Data are available at NAR Online.

ACKNOWLEDGEMENTS

We thank M.C. Guerin for the quantitative PCR facility (IFR122). This work was supported by the CNRS, SIDACTION, ANRS and the Ministère de la Recherche (ACI) to M.M. L.H. was supported by fellowship from SIDACTION, F.S. by CNRS and S.M. by the Ministère de la Recherche (ACI). Funding to pay the Open Access publication charge was provided by CNRS.

Conflict of interest statement. None declared.

REFERENCES

1. Poole,E., Strappe,P., Mok,H.P., Hicks,R. and Lever,A.M. (2005) HIV-1 Gag-RNA interaction occurs at a perinuclear/centrosomal site; analysis by confocal microscopy and FRET. *Traffic*, **6**, 741–755.
2. D'Souza,V. and Summers,M.F. (2005) How retroviruses select their genomes. *Nat. Rev. Microbiol.*, **3**, 643–655.
3. Paillart,J.C., Marquet,R., Skripkin,E., Ehresmann,C. and Ehresmann,B. (1996) Dimerization of retroviral genomic RNAs: structural and functional implications. *Biochimie*, **78**, 639–653.
4. Amarasinghe,G.K., De Guzman,R.N., Turner,R.B. and Summers,M.F. (2000) NMR structure of stem-loop SL2 of the HIV-1 psi RNA packaging signal reveals a novel A-U-A base-triple platform. *J. Mol. Biol.*, **299**, 145–156.
5. Hayashi,T., Shioda,T., Iwakura,Y. and Shibuta,H. (1992) RNA packaging signal of human immunodeficiency virus type 1. *Virology*, **188**, 590–599.
6. Luban,J. and Goff,S.P. (1994) Mutational analysis of cis-acting packaging signals in human immunodeficiency virus type 1 RNA. *J. Virol.*, **68**, 3784–3793.
7. McBride,M.S., Schwartz,M.D. and Panganiban,A.T. (1997) Efficient encapsidation of human immunodeficiency virus type 1 vectors and further characterization of cis elements required for encapsidation. *J. Virol.*, **71**, 4544–4554.
8. Helga-Maria,C., Hammarskjold,M.L. and Rekosh,D. (1999) An intact TAR element and cytoplasmic localization are necessary for efficient packaging of human immunodeficiency virus type 1 genomic RNA. *J. Virol.*, **73**, 4127–4135.
9. Clever,J.L., Mirandar,D.Jr and Parslow,T.G. (2002) RNA structure and packaging signals in the 5′ leader region of the human immunodeficiency virus type 1 genome. *J. Virol.*, **76**, 12381–12387.
10. Russell,R.S., Hu,J., Laughrea,M., Wainberg,M.A. and Liang,C. (2002) Deficient dimerization of human immunodeficiency virus type 1 RNA caused by mutations of the u5 RNA sequences. *Virology*, **303**, 152–163.
11. Liang,C., Hu,J., Russell,R.S., Kameoka,M. and Wainberg,M.A. (2004) Spliced human immunodeficiency virus type 1 RNA is reverse transcribed into cDNA within infected cells. *AIDS Res. Hum. Retroviruses*, **20**, 203–211.
12. Berkowitz,R., Fisher,J. and Goff,S.P. (1996) RNA packaging. *Curr. Top. Microbiol. Immunol.*, **214**, 177–218.
13. Hill,M.K., Shehu-Xhilaga,M., Campbell,S.M., Poumbourios,P., Crowe,S.M. and Mak,J. (2003) The dimer initiation sequence stem-loop of human immunodeficiency virus type 1 is dispensable for viral replication in peripheral blood mononuclear cells. *J. Virol.*, **77**, 8329–8335.
14. Clever,J.L. and Parslow,T.G. (1997) Mutant human immunodeficiency virus type 1 genomes with defects in RNA dimerization or encapsidation. *J. Virol.*, **71**, 3407–3414.
15. Russell,R.S., Hu,J., Beriault,V., Mouland,A.J., Laughrea,M., Kleiman,L., Wainberg,M.A. and Liang,C. (2003) Sequences downstream of the 5′ splice donor site are required for both packaging and dimerization of human immunodeficiency virus type 1 RNA. *J. Virol.*, **77**, 84–96.
16. Roy,B.B., Russell,R.S., Turner,D. and Liang,C. (2006) The T12I mutation within the SP1 region of Gag restricts packaging of spliced viral RNA into human immunodeficiency virus type 1 with mutated RNA packaging signals and mutated nucleocapsid sequence. *Virology*, **344**, 304–314.
17. Purcell,D.F. and Martin,M.A. (1993) Alternative splicing of human immunodeficiency virus type 1 mRNA modulates viral protein expression, replication, and infectivity. *J. Virol.*, **67**, 6365–6378.
18. Wodrich,H. and Krausslich,H.G. (2001) Nucleocytoplasmic RNA transport in retroviral replication. *Results Probl. Cell Differ.*, **34**, 197–217.
19. Muriaux,D. and Rein,A. (2003) Encapsidation and transduction of cellular genes by retroviruses. *Front Biosci.*, **8**, D135–142.
20. Onafuwa-Nuga,A.A., Telesnitsky,A. and King,S.R. (2006) 7SL RNA, but not the 54-kd signal recognition particle protein, is an abundant component of both infectious HIV-1 and minimal virus-like particles. *RNA*, **12**, 542–546.
21. Giles,K.E., Caputi,M. and Beemon,K.L. (2004) Packaging and reverse transcription of snRNAs by retroviruses may generate pseudogenes. *RNA*, **10**, 299–307.
22. Muriaux,D., Mirro,J., Harvin,D. and Rein,A. (2001) RNA is a structural element in retrovirus particles. *Proc. Natl Acad. Sci. USA*, **98**, 5246–5251.
23. Paillart,J.C., Berthoux,L., Ottmann,M., Darlix,J.L., Marquet,R., Ehresmann,B. and Ehresmann,C. (1996) A dual role of the putative RNA dimerization initiation site of human immunodeficiency virus type 1 in genomic RNA packaging and proviral DNA synthesis. *J. Virol.*, **70**, 8348–8354.
24. Willey,R.L., Smith,D.H., Lasky,L.A., Theodore,T.S., Earl,P.L., Moss,B., Capon,D.J. and Martin,M.A. (1988) *In vitro* mutagenesis identifies a region within the envelope gene of the human immunodeficiency virus that is critical for infectivity. *J. Virol.*, **62**, 139–147.
25. Smagulova,F., Maurel,S., Morichaud,Z., Devaux,C., Mougel,M. and Houzet,L. (2005) The highly structured encapsidation signal of MuLV RNA is involved in the nuclear export of its unspliced RNA. *J. Mol. Biol.*, **354**, 1118–1128.
26. Houzet,L., Battini,J., Bernard,E., Thibert,V. and Mougel,M. (2003) A new retroelement constituted by a natural alternatively spliced RNA of murine replication-competent retroviruses. *EMBO J.*, **22**, 4866–4875.
27. Bagnarelli,P., Valenza,A., Menzo,S., Sampaolesi,R., Varaldo,P.E., Butini,L., Montroni,M., Perno,C.F., Aquaro,S. *et al.* (1996) Dynamics and modulation of human immunodeficiency virus type 1 transcripts *in vitro* and *in vivo*. *J. Virol.*, **70**, 7603–7613.
28. Levesque,K., Halvorsen,M., Abrahamyan,L., Chatel-Chaix,L., Poupon,V., Gordon,H., DesGroseillers,L., Gatignol,A. and Mouland,A.J. (2006) Trafficking of HIV-1 RNA is mediated by heterogeneous nuclear ribonucleoprotein A2 expression and impacts on viral assembly. *Traffic*, **7**, 1177–1193.
29. Onafuwa-Nuga,A.A., King,S.R. and Telesnitsky,A. (2005) Nonrandom packaging of host RNAs in Moloney murine leukemia virus. *J. Virol.*, **79**, 13528–13537.
30. Sakuragi,J., Ueda,S., Iwamoto,A. and Shioda,T. (2003) Possible role of dimerization in human immunodeficiency virus type 1 genome RNA packaging. *J. Virol.*, **77**, 4060–4069.
31. Das,A.T., Klaver,B. and Berkhout,B. (1998) The 5′ and 3′ TAR elements of human immunodeficiency virus exert effects at several points in the virus life cycle. *J. Virol.*, **72**, 9217–9223.
32. McBride,M.S. and Panganiban,A.T. (1997) Position dependence of functional hairpins important for human immunodeficiency virus type 1 RNA encapsidation *in vivo*. *J. Virol.*, **71**, 2050–2058.
33. Harrich,D., Hooker,C.W. and Parry,E. (2000) The human immunodeficiency virus type 1 TAR RNA upper stem-loop plays distinct roles in reverse transcription and RNA packaging. *J. Virol.*, **74**, 5639–5646.
34. Mougel,M., Zhang,Y. and Barklis,E. (1996) *Cis*-active structural motifs involved in specific encapsidation of Moloney murine leukemia virus RNA. *J. Virol.*, **70**, 5043–5050.
35. Fisher,J. and Goff,S.P. (1998) Mutational analysis of stem-loops in the RNA packaging signal of the Moloney murine leukemia virus. *Virology*, **244**, 133–145.
36. Paillart,J.C., Shehu-Xhilaga,M., Marquet,R. and Mak,J. (2004) Dimerization of retroviral RNA genomes: an inseparable pair. *Nat. Rev. Microbiol.*, **2**, 461–472.
37. Lever,A.M. (2000) HIV RNA packaging and lentivirus-based vectors. *Adv. Pharmacol.*, **48**, 1–28.
38. Paillart,J.C., Marquet,R., Skripkin,E., Ehresmann,B. and Ehresmann,C. (1994) Mutational analysis of the bipartite dimer linkage structure of human immunodeficiency virus type 1 genomic RNA. *J. Biol. Chem.*, **269**, 27486–27493.
39. Laughrea,M. and Jette,L. (1997) HIV-1 genome dimerization: kissing-loop hairpin dictates whether nucleotides downstream of the 5′ splice junction contribute to loose and tight dimerization of human immunodeficiency virus RNA. *Biochemistry*, **36**, 9501–9508.
40. Berkowitz,R.D., Hammarskjold,M.L., Helga-Maria,C., Rekosh,D. and Goff,S.P. (1995) 5′ regions of HIV-1 RNAs are not sufficient for encapsidation: implications for the HIV-1 packaging signal. *Virology*, **212**, 718–723.

41. Kaye,J.F., Richardson,J.H. and Lever,A.M. (1995) cis-Acting sequences involved in human immunodeficiency virus type 1 RNA packaging. *J. Virol.*, **69**, 6588–6592.
42. Parolin,C., Dorfman,T., Palu,G., Gottlinger,H. and Sodroski,J. (1994) Analysis in human immunodeficiency virus type 1 vectors of cis-acting sequences that affect gene transfer into human lymphocytes. *J. Virol.*, **68**, 3888–3895.
43. Geigenmuller,U. and Linial,M.L. (1996) Specific binding of human immunodeficiency virus type 1 (HIV-1) Gag-derived proteins to a 5′ HIV-1 genomic RNA sequence. *J. Virol.*, **70**, 667–671.
44. Mouland,A.J., Mercier,J., Luo,M., Bernier,L., DesGroseillers,L. and Cohen,E.A. (2000) The double-stranded RNA-binding protein Staufen is incorporated in human immunodeficiency virus type 1: evidence for a role in genomic RNA encapsidation. *J. Virol.*, **74**, 5441–5451.
45. Gallego,J., Greatorex,J., Zhang,H., Yang,B., Arunachalam,S., Fang,J., Seamons,J., Lea,S., Pomerantz,R.J. *et al.* (2003) Rev binds specifically to a purine loop in the SL1 region of the HIV-1 leader RNA. *J. Biol. Chem.*, **278**, 40385–40391.
46. Henriet,S., Richer,D., Bernacchi,S., Decroly,E., Vigne,R., Ehresmann,B., Ehresmann,C., Paillart,J.C. and Marquet,R. (2005) Cooperative and specific binding of Vif to the 5′ region of HIV-1 genomic RNA. *J. Mol. Biol.*, **354**, 55–72.
47. Saurya,S., Lichtenstein,Z. and Karpas,A. (2005) Defective rev response element (RRE) and rev gene in HAART treated AIDS patients with discordance between viral load and CD4+ T-cell counts. *J. Clin. Virol.*, **33**, 324–327.
48. Wang,L.H. (1987) The mechanism of transduction of proto-oncogene c-src by avian retroviruses. *Mutat. Res.*, **186**, 135–147.
49. Sinn,P.L., Sauter,S.L. and McCray,P.B.Jr (2005) Gene therapy progress and prospects: development of improved lentiviral and retroviral vectors – design, biosafety, and production. *Gene Ther.*, **12**, 1089–1098.